Available online at www.sciencedirect.com
SCIENCE DIRECT®
Physics Letters B 594 (2004) 105–117
PHYSICS LETTERS B
www.elsevier.com/locate/physletb

Subthreshold photoproduction of charm

M.A. Braun [1], B. Vlahovic

North Carolina Central University, Durham, NC, USA

Received 6 April 2004; received in revised form 6 May 2004; accepted 7 May 2004

Available online 11 June 2004

Editor: P.V. Landshoff

Abstract

Charm photoproduction rates off nuclei below the nucleon threshold are estimated using the phenomenologically known structure functions both for $x > 1$. The rates rapidly fall below the threshold from values ~ 10 pb for Pb close to the threshold (at 7.5 GeV) to ~ 1 pb at 6 GeV.

1. Introduction

In view of the envisaged upgrade of the CEBAF facility up to 12 GeV it becomes important to have relatively secure predictions about the production rates of charm on nuclear targets below the threshold for the nucleon target. This Letter aims at such predictions. We try to estimate the subthreshold production rate from the gluon distribution in the appropriate kinematical region. The latter will be related to the nuclear structure function in the region $x > 1$, for which we shall use the existing (scarce) experimental data. These data are only known at x quite close to unity, so our procedure necessarily involves their extrapolation to higher x, which involves considerable uncertainty in view of poor knowledge of the slope in x. Also the relation between the structure function and gluon density depends on the assumptions made about the initial parton densities at the start of the DGLAP evolution, which have not been studied for $x > 1$. Finally, as we shall see, in the low energy region the charm production rate involves the gluon distribution not only in x (collinear factorization) but also in both x and $k_\perp^2$ ($k_\perp$ factorization). In view of the approximate character of our calculations we shall use the simplest approximation about the structure of this combined distribution, assuming the dependence on x and $k_\perp$ factorized. With all these uncertainties, we hope to be able to predict the rates up to factor 2–3.[2]

From the start it has to be recalled that the dynamical picture of charm production at energies close to the threshold is much more complicated than at high energies. Due to smallness of the production rate, some contribution to it may originate from such non-standard mechanisms as liberation of intrinsic charm. In this Letter

E-mail address: mijail@fpaxp1.usc.es (M.A. Braun).

[1] Permanent address: Department of High Energy Physics, St. Petersburg University, 198504 St. Petersburg, Russia.

[2] Some crude estimates were earlier reported in [2]. Their order agrees with the present calculations at energies not too close to the threshold.

0370-2693
doi:10.1016/j.physletb.2004.05.013

we do not discuss this latter mechamism. Estimates of intrinsic charm contribution are very uncertain but typically they lead to a rather small value (see, e.g., [1]). Staying within the more common picture, in which charm is produced due to fusion of the photon with gluons of the target, the main problem is that in the immediate vicinity of the threshold the standard fusion with a single gluon becomes overshadowed by multiple gluon exchanges [3] and formation of colourless bound states with lower mass, as compared to open charm [4].

Assuming that the threshold value of the scaling variable for the produced $c\bar{c}$ pair of mass M is $x = 1$, one finds that the relative weight of multigluon exchanges is measured by a factor

$$r = 1/\left[(1-x)^2 R^2 M^2\right],$$

where $R \sim 1/\Lambda_{\mathrm{QCD}} \sim 1$ fm [3]. Numerically this factor is $\sim 1/[225\,(1-x)^2]$, so that already at $1-x \sim 0.1$ each new gluon exchange is damped by at least $1/2$. In fact this damping is stronger due to the fact that such an exchange involves a smaller strong coupling constant, taken at the scale M. So multiple gluon exchanges play their role only quite close to the threshold. In Appendix A, on a simple example of a mesonic target, we find that, in terms of energy of the reaction, already at distances around 0.3 GeV from the threshold multiple gluon exchanges give a small contribution as compared to the single gluon exchange.

The same argument can be applied to nuclear targets. Take the deuteron and consider it as a bound stae of six quarks. In terms of x the threshold is now at $x = 2$. Obviously, in the interval $1 < x < 2$ the heavy quarks have to collect their longitudinal momenta from quarks belonging to different nucleons inside the deuteron. This implies that in any case the two nucleons have to be located at a small distance of the order $1/M$ in the deuteron, which by itself makes the production rate very small. Now consider the behaviour of this rate close to the deuteron threshold $x = 2$ and compare contributions from a single and multiple gluon exchanges. Each new gluon exchange will again involve the same factor r relative to the single gluon exchange contribution. As a result, similar to the the nucleon target case, already at small distances of the order 0.3–0.4 GeV from the deuteron threshold one may neglect the contribution from multiple gluon exchanges, at least for comparatively crude estimates.

This argument forms the basis of our treatment. We shall study charm production below the normal threshold for the nucleon target but above the threshold for the deuteron target, at not too small distances from the thresholds, where all effects due to multiple gluon exchanges are hopefully small. To be more concrete, taking the charmed quark mass $m_c = 1.55$ GeV, we have the threshold of open charm photoproduction on the proton target at the incident photon energy $E_1^{\mathrm{th}} = 8.2$ GeV and on the deuteron target at $E_2^{\mathrm{th}} = 5.6$ GeV. As we shall argue (see Appendix A), our treatment is hopefully valid at incident photon energies E in the interval $6.0 < E < 7.8$ GeV. Closer to the thresholds multigluon exchanges and bound state formation may change our predictions considerably.

Neglecting multiple gluon exchanges, as mentioned at the beginning, subthreshold production will be determined by the gluon distribution in the "cumulative" region ($x > 1$ at large energies or massless target). So our task will be to estimate this distribution from the experimental data on the nuclear structure function at $x > 1$. This will be done using the standard DGLAP equations at $x > 1$ assuming certain initial distributions. We mostly rely on the assumption that at certain low $Q^2 = Q_0^2$ the nucleons consist only of valence quarks, all other distributions going to zero [5]. However, we also studied the influence of non-zero initial sea and gluon distributions. Inclusion of a non-zero sea distribution does not change our results in any significant way. Inclusion of a non-zero gluon distribution enhances the rates without changing their form. In the limiting (improbable to our mind) case when the initial gluon distribution at $x > 1$ is equal to the valence one the rates are doubled.

2. Kinematics and cross-sections

2.1. The charm production cross-section

Consider the exclusive process

$$\gamma + A \to C\bar{C} + A^*, \tag{1}$$

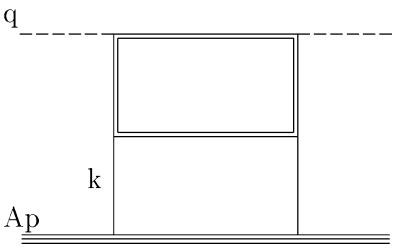

Fig. 1. The forward scattering amplitude corresponding to reaction (1). Heavy quarks are shown by double lines.

where A is the target nucleus of mass m_A and A^* is the recoil nuclear system of mass m_A^*. We denote the total mass of the $C\bar{C}$ system as M. Obviously, $M \geqslant 2m_c$, where m_c is the mass of the C-quark, which we take as 1.5 GeV. The inclusive cross-section for charm photoproduction is obtained after summing over all states of the recoil nuclear system.

We choose a reference system in which the target nucleus with momentum Ap is at rest and the incoming photon with momentum q is moving along the z-axis in the opposite direction, so that $q_+ = q_\perp = 0$. The photoproduction cross-section corresponding to (1) is then obtained via the imaginary part of the diagram in Fig. 1 as

$$\sigma_{A\to A^*} = A\int \frac{d^4k}{(2\pi)^3}\delta\big((Ap-k)^2 - m_A^{*2}\big)x\left(\frac{\Gamma_{AA^*}(k^2)}{k^2}\right)^2\sigma_g\big(M^2,k^2\big). \tag{2}$$

Here $\Gamma_{AA^*}(k^2)$ is the vertex for gluon emission from the target; $\sigma_g(M^2,k^2)$ is the photoproduction cross-section off the virtual gluon of momentum k. We have also introduced the scaling variable for the gluon as $x = k_+/p_+$. Due to $q_+ = 0$ this is also the scaling variable for the observed charm. Note that this definition, which is standard at large energies and produced masses, is not at all standard at moderate scales. In particular, this x does not go to unity at the threshold for the nucleon target. Rather the limits for its variation converge to a common value 0.76. For the nuclear targets with $A \gg 1$ its minimal value at the nucleon threshold is well below unity (~ 0.64). One should have this in mind when associating this x with the gluon distribution: it follows that for a nuclear target, for energies going noticeably below the nucleon threshold, the cumulative region (prohibited for the free nucleons kinematics) includes not only values of x above unity but also a part of the region $x < 1$.

We use the δ-function to integrate over k_- to obtain the cross-section (2) as

$$\sigma_{A\to A^*} = A\int \frac{dx\,d^2k_\perp}{2(A-x)(2\pi)^3}\left(\frac{\Gamma_{AA^*}(k^2)}{k^2}\right)^2\sigma_g\big(M^2,k^2\big). \tag{3}$$

In these variables we find

$$M^2 = xs_1 + k^2, \quad s_1 = 2pq, \tag{4}$$

$$k^2 = xAm^2 - \frac{x}{A-x}m_A^{*2} - \frac{A}{A-x}k_\perp^2, \tag{5}$$

where we have put $p^2 = m^2$, the nucleon mass squared, neglecting the binding.

The limits of integration in (3) are determined by the condition $M^2 \geqslant 4m_c^2$, which leads to

$$x\big(s_1 + Am^2\big) - \frac{x}{A-x}m_A^{*2} - \frac{A}{A-x}k_\perp^2 - 4m_c^2 \geqslant 0. \tag{6}$$

Since $k_\perp^2 \geqslant 0$, one gets

$$x\big(s_1 + Am^2\big) - \frac{x}{A-x}m_A^{*2} - 4m_c^2 \geqslant 0, \tag{7}$$

from which one finds the limits of integration in x for the transition $A \to A^*$:

$$x_1^{A\to A^*} \leqslant x \leqslant x_2^{A\to A^*}, \tag{8}$$

where

$$x_{1,2}^{A\to A^*} = \frac{1}{2s}\Big(As - m_A^{*2} + 4m_c^2 \pm \sqrt{\big[As - (m_A^* + 2m_c)^2\big]\big[As - (m_A^* - 2m_c)^2\big]}\Big) \tag{9}$$

and $s = s_1 + Am^2$. The limits of integration in $k_\perp$ at a given x are determined by (6).

Using (5) we may pass from the integration variable $k_\perp^2$ to $|k^2|$. Summing over all states of the recoiling nucleus A^* we get

$$\sigma_A = \int\limits_{x_1^{(A)}}^{x_2^{(A)}} x\,dx \int\limits_{|k^2|_{\min}}^{xs_1 - 4m_c^2} d\big|k^2\big|\,\sigma_g\big(xs_1 - \big|k^2\big|, k^2\big)\rho\big(x, \big|k^2\big|\big), \tag{10}$$

where

$$\rho\big(x, \big|k^2\big|\big) = \frac{\pi}{2(2\pi)^3}\sum_{A^*}\left(\frac{\Gamma_{AA^*}(k^2)}{k^2}\right)^2, \tag{11}$$

$$\big|k^2\big|_{\min} = \frac{A}{A-x}x^2m^2, \tag{12}$$

and $x_{1,2}^{(A)}$ determined by (9) with m_A^* put to its minimal value $m_A^* = m_A = Am$.

The threshold energy corresponds to $x_1^{(A)} = x_2^{(A)}$ or $As = (Am + 2m_c)^2$. In terms of the photon energy E we have $s_1 = 2mE$ and the threshold energy is found to be

$$E_A^{\text{th}} = 2m_c\left(1 + \frac{1}{A}\frac{m_c}{m}\right). \tag{13}$$

It steadily falls with A from the nucleon target threshold. With $m_c = 1.55$ GeV we find (in GeV):

$$E_1^{\text{th}} = 8.2, \quad E_2^{\text{th}} = 5.6, \quad E_3^{\text{th}} = 4.8, \quad E_{12}^{\text{th}} = 3.5, \quad E_{207}^{\text{th}} = 3.1. \tag{14}$$

2.2. High-energy limit

To interprete ρ in Eq. (10) it is instructive to study its high-energy limit, which corresponds to taking $s_1 \gg m_c^2$ and both quantities much greater than the nucleon mass. Assuming that the effective values of the gluon virtuality are limited (and small) one then gets for the nucleon target ($A = 1$)

$$\sigma_1 = \int\limits_{4m_c^2/s_1}^{1} x\,dx\,\sigma_g(xs_1)\int\limits_0^{xs_1} d\big|k^2\big|\,\rho\big(x, \big|k^2\big|\big). \tag{15}$$

Here we also neglect the off-mass-shellness of the cross-section off the gluon, considering $|k^2| \ll 4m_c^2$. The obtained formula is precisely the standard collinear factorization formula with the identification

$$xg\big(x, M^2\big) = \int\limits_0^{M^2} d\big|k^2\big|\,x\rho\big(x, \big|k^2\big|\big). \tag{16}$$

Thus the quantity $\rho(x, |k^2|)$ obviously has a meaning of the double distribution of gluons in x and $|k^2|$.

3. The gluon distribution $\rho(x, |k^2|)$

To find the double distribution of gluons in x and $|k^2|$ one may be tempted to use (16) and simply differentiate $xg(x, M^2)$ in $M^2 = |k^2|$. However, (16) is only true for $x \ll 1$. At finite x the derivative $dg(x, m^2)/dM^2$ is not positive and cannot be interpreted as the double gluonic distribution.

To avoid this problem, we choose a different, somewhat simplified approach. We assume a simple factorizable form for the double density $\rho(x, |k^2|)$ and choose the $|k^2|$-dependence in accordance with the perturbation theory, with an infrared cutoff in the infrared region:

$$\rho\big(x, |k^2|\big) = \frac{a(x)}{|k^2| + \Lambda^2}. \tag{17}$$

Function $a(x)$ can be obtained matching (17) with the observed $xg(x, M^2)$ at a particular point M_0^2. Since we are interested in the threshold region, we take $M_0 = 2m_c$ to finally obtain

$$\rho\big(x, |k^2|\big) = \frac{g(x, 4m_c^2)}{\ln(4m_c^2/\Lambda^2 + 1)} \frac{1}{|k^2| + \Lambda^2}. \tag{18}$$

The recipe (18) amounts to taking in (16) ρ dependent also on M^2, with the latter dependence factorized. Our calculations show that the results are rather weakly dependent of the infrared cutoff chosen in the interval 0.4–0.7 GeV.

For the nuclei in the cumulative region

$$x_1^{(A)} < x < x_2^{(A)} \quad \text{outside} \quad x_1^{(1)} < x < x_2^{(1)}, \tag{19}$$

the gluon distribution may be estimated using, first, the existing data for the nuclear structure functions in this region and, second, the hypothesis that at sufficiently low $Q^2 = Q_0^2$ the sea and gluon distributions vanish and hadrons become constructed exclusively of valence quarks. Then one can find the gluon distribution at a given Q^2 from the standard DGLAP evolution equation with the quark distributions determined from the experimental data on the structure functions at $x > 1$ and evolved back to $Q^2 = Q_0^2$. In practice we took the initial valence distributions in carbon at $Q^2 = Q_0^2$ in the form

$$u\big(x, Q_0^2\big) = d\big(x, Q_0^2\big) = ae^{-bx} \tag{20}$$

and the rest of the distributions equal to zero. Then we calculated the carbon structure function at $x > 1$ and Q^2 in correspondence with the data of [6] and chose the parameters a and b to fit the data. With thus chosen a and b we finally calculated the gluon distribution in carbon at the scale $4m_c^2$. Our obtained gluon distributions in carbon for $Q_0 = 0.4$ and 0.7 GeV/c are shown in Fig. 2 for $1 < x < 2$. As one observes, the dependence on the choice of Q_0 is very weak in this interval. The slopes result equal to 11.4 ($Q_0 = 0.4$ GeV/c) and 11.2 ($Q_0 = 0.7$). The distribution for other nuclei was taken from the A-dependence, chosen in accordance with the experimental data for hadron production at $x > 1$ as $\propto A^{1+0.3x}$ [7].

The assumption that at $Q^2 = Q_0^2$ the sea and gluon distributiion vanish may appear to be too radical. So we studied the effect of non-zero sea and gluon distributions at the beginning of the evolution. Inclusion of a non-zero initial sea distribution of a reasonable size does not change our results in any way. Inclusion of a non-zero initial gluon distribution enhances the gluon density at $4m_c^2$. Taking the initial gluon distribution of the same form (20) with an extra coefficient κ we found the gluon density at $4m_c^2$ enhanced by factor $\sim (1 + \kappa)$. In Fig. 2 the upper curve shows this gluon density for the case $\kappa = 1$ (improbable to our mind). It is roughly doubled.

In the non-cumulative region $x_1^{(1)} < x < x_2^{(1)}$ at low enough x one could take the gluon distribution as $g_A(x, 4m_c^2) = Ag_1(x, 4m_c^2)$, where $g_1(x, Q^2)$ is the gluon distribution in the proton (thus neglecting the EMC effect in the first approximation). However, this is obviously not satisfactory at $x < 1$ but close to unity. On the threshold $x = 1$ and in a certain interval of x below unity the nuclear gluon density determined from the cumulative

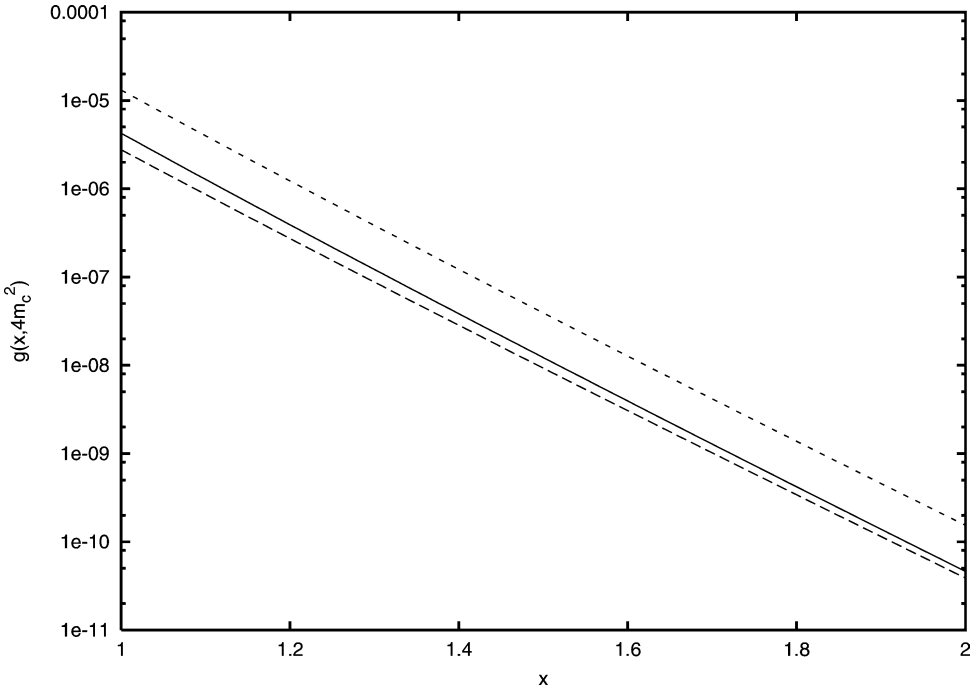

Fig. 2. The cumulative ($x > 1$) gluon distributions in carbon at $Q^2 = 4m_c^2$. The two lower curves from bottom to top correspond to $Q_0 = 0.7(0.4)$ GeV/c. The upper curve corresponds to the case when the initial gluon distribution at $Q_0 = 0.4$ GeV/c is equal to the valence ones.

structure function by the procedure described above remains much greater than $Ag_1(x, 4m_c^2)$. Thus one has to use this gluon density also in a part of the interval $x < 1$ down to the value of x at which $Ag_1(x, 4m_c^2)$ begins to dominate. In fact all the integration region of $x < 1$ in Eq. (10) lies inside this interval. So our calculations do not need the gluon distribution inside the proton at all and are totally based on the experimental nuclear structure functions at both $x > 1$ and $x < 1$ but close to unity.

4. Numerical results

The cross-section (10) involves the photon–gluon fusion cross-section σ_g off mass shell. The integration over the gluon virtuality starts from $|k^2| \sim m^2$. If one assumes $m/M \to 0$ then the bulk of the contribution will come from the region of small $|k^2|$ (with a logarithmic precision). In reality m/M is not so small. However, to simplify our calculations, as a first approximation, we have taken the photon–gluon cross-section on the mass shell, where it is known to be [8]

$$\sigma_g\big(M^2\big) = \pi\alpha_{\rm em}\alpha_s e_c^2 \frac{1}{M^4}\int\limits_{t_1}^{t_2} dt\left[\frac{t}{u} + \frac{u}{t} + \frac{4m_c^2M^2}{tu}\left(1 - \frac{m_c^2M^2}{tu}\right)\right]. \tag{21}$$

Here e_c is the quark charge in units e, $u = -M^2 - t$ and the limits $t_{1,2}$ are given by

$$t_{1,2} = -\frac{M}{2}\Big[M \pm \sqrt{M^2 - 4m_c^2}\Big]. \tag{22}$$

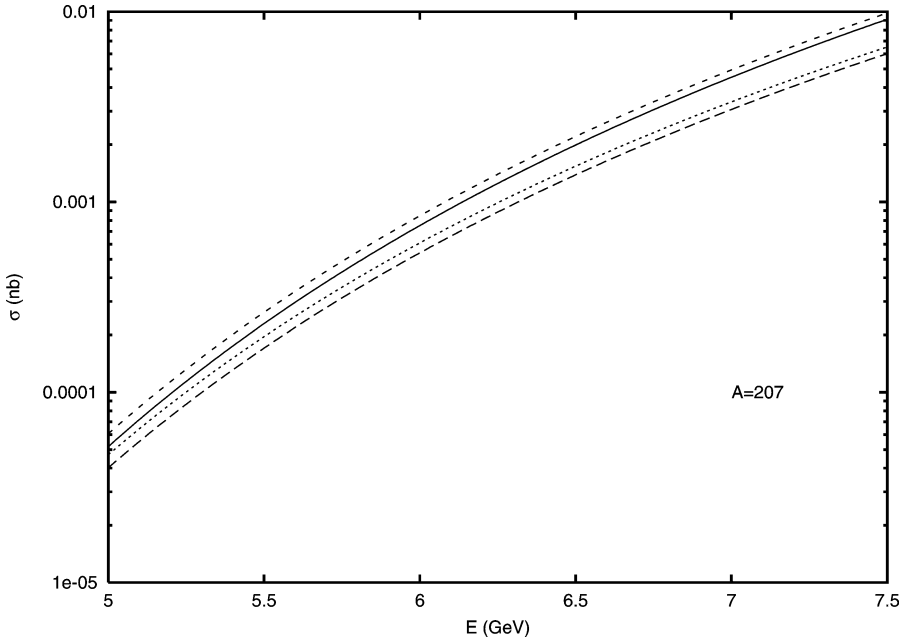

Fig. 3. The charm photoproduction subthreshold cross-sections off Pb for different choice of parameters Λ and Q_0. Curves from bottom to top correspond to $(\Lambda, Q_0) = (0.4, 0.7), (0.7, 0.7), (0.4, 0.4)$ and $(0.7, 0.4)$ GeV/c. The uppermost curve corresponds to the case when the initial gluon distribution at $Q_0 = 0.4$ GeV/c is equal to the valence ones (with $\Lambda = 0.4$ GeV/c).

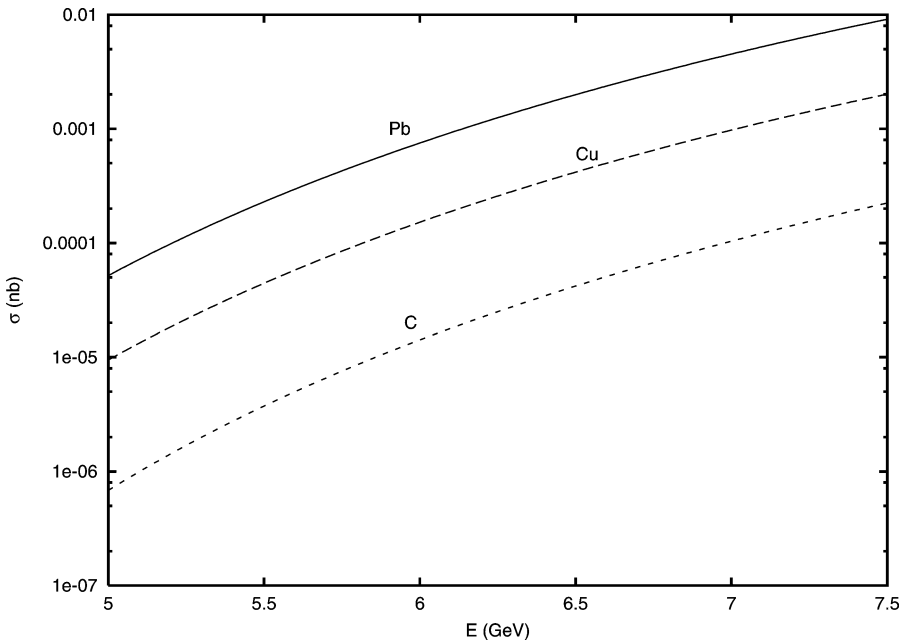

Fig. 4. The charm photoproduction subthreshold cross-sections for different targets. Curves from bottom to top correspond to $A = 12$, 64 and 207.

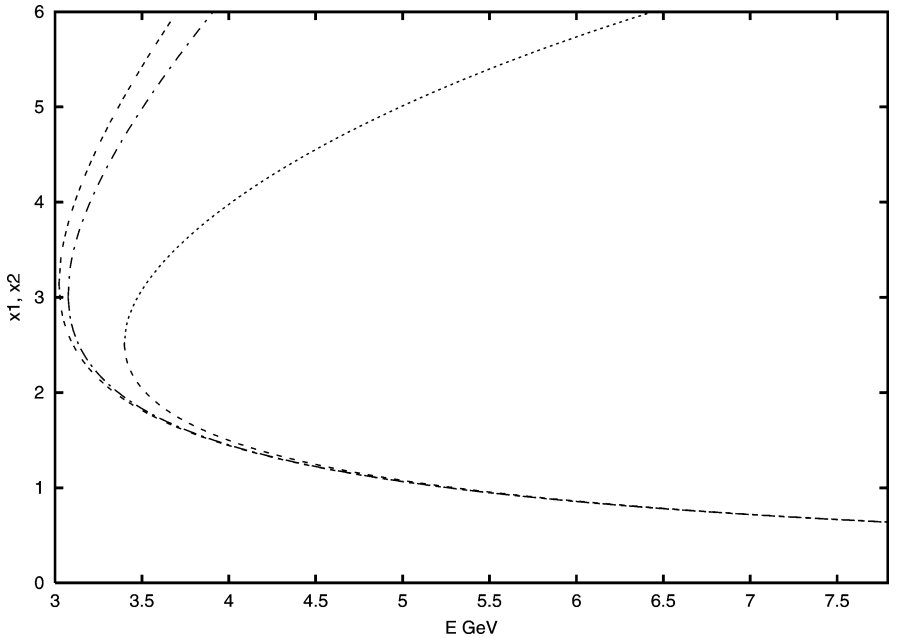

Fig. 5. The limits of x-integration for different photon energies and nuclear targets. Curves from bottom to top correspond to $A = 12$, 64 and 207.

We take the strong coupling constant $\alpha_s = 0.3$.

Our gluon distribution depends on two parameters: the infrared cutoff Λ in (19) and the value of Q_0, at which the sea and gluon distributions die out. The order of both is well determined, but still one can vary them to some degree. In our calculations we took both Λ and Q_0 equal to 0.4 or 0.7 GeV/c.

With these values for the parameters we obtain the cross-sections for charm photoproduction on Pb shown in Fig. 3. As one observes, the dependence on both Λ and Q_0 is relatively weak: in the whole range of their variation the cross-sections change by less than 30%. We have also shown the cross-section for the case when at the initial $Q^2 = Q_0^2$ there exists a non-zero gluon distribution of the same form and magnitude as the valence one (the upper curve, $Q_0 = \Lambda = 0.4$ GeV/c). As with the gluon density, the resulting cross-section is then roughly doubled.

Fig. 4 illustrates the A-dependence of the cross-sections (with $\Lambda = Q_0 = 0.4$ GeV/c). To have the idea of the number of nucleons which have to interact together to produce charm at fixed energy below threshold we show the limits of intergation x_1 and x_2 in Fig. 5.

As expected the cross-sections rapidly fall for energies below threshold. Their energy dependence cannot be fit with a simple exponential (in fact they fall faster than the exponential). As to the aboslute values, for Pb the cross-section fall from ~ 10 pb immediately below the threshold down to ~ 1 pb at $E = 6$ GeV. The A-dependence is close to linear.

5. Discussion

We have estimated charm photoproduction rates for nuclear targets below the nucleon target threshold. Several assumption and simplifications have been used.

The estimates require knowledge of the gluon distribution in both x and $k_\perp^2$ in a wide region of the momenta including the confinement region. Our estimates were based on a simple factorization assumption and introduction of an infrared cutoff. However, the cutoff dependence was found to be weak for variations of the cutoffs in a

reasonable interval. Another approximation has been to take the photon–gluon fusion cross-section on its mass-shell. We are of the opinion that both these technical approximation are not very serious The second one can easily be dropped for the price of considerable complication of the calculation. As to the first one, the corresponding double distributions are now widely discussed in the framework of the combined BFKL + DGLAP evolution equation [9] and in principle the results of this discussion can be used to somewhat improve our estimates.

At the present stage we consider such an improvement preliminary, because there are three points which, in our opinion, introduce much more uncertainty. These are poor experimental knowledge of the nuclear structure functions at x substantially larger than unity, certain arbitrariness in the choice of initial parton distributions for the DGLAP evolution and, finally, insecure estimates of the intrinsic charm contribution. From each of these points, in our opinion, one may expect a change in the rate up tp 100%. As a result we expect our rates to be true up to factor 2–3. Note that both intrinsic charm and non-zero initial gluon distribution enhance the rate. So in this respect our estimates correspond to the lower bound for the cross-section.

In our study we assumed the standard mechanism of charm production via gluon–photon fusion (a single gluon exchange between light and heavy quarks). It can be shown that this mechanism dominates, provided one is not too close to the threshold (see Appendix A).

Acknowledgements

M.A.B. is thankful to the Faculty of Science of the NCCU for hospitality.

Appendix A. Multiple gluon exchange

A.1. Kinematics and phase volume

To study the relative weight of multiple gluon exchange we consider a simplified picture with a mesonic target composed of a light quark and antiquark of mass μ. We neglect the binding, so that the meson mass is just 2μ. We shall compare contributions to heavy flavour production of the three amplitudes Fig. 6(a)–(c). Amplitude (a) corresponds to a single gluon exchange between light and heavy quarks, amplitudes (b) and (c) to double gluon exchange. We use the light-cone variables and denote $k_{i+} = z_i p_+$, $p_{i+} = x_i p_+$, $i = 1, 2$.

The phase volume for the reaction is given by

$$dV = \frac{1}{16(2\pi)^8} \frac{d^3k_1\, d^3p_1\, d^3p_2}{z_1 z_2 x_1 x_2} \delta(R_e - R), \tag{A.1}$$

where $d^3k_1 = dz_1\, d^2k_{1\perp}$, etc., and the δ function refers to conservation of the light-cone energy (the "$-$" component of the momentum). Its argument contains the external energy $R_e = 2pq + 4\mu^2 = 2\mu E + 4\mu^2$, and the energy of the produced particles $R = \sum_{i=1}^{2} (m_{c,i\perp}^2/z_i + \mu_{i\perp}^2/x_i)$. The minimal value of R determining the production threshold occurs at

$$z_i = z_0 = \frac{m_c}{m_c + \mu}, \qquad x_i = x_0 = \frac{\mu}{m_c + \mu}, \qquad k_{i\perp} = p_{i\perp} = 0, \quad i = 1, 2, \tag{A.2}$$

and is equal to $\min R = R_0 = 2(m_c + \mu)^2$.

We shall study our amplitudes near the threshold, so that x_i will be small and z_i will be close to unity. We put $z_i = z_0 + \zeta_i$, $x_i = x_0 + \xi_i$, $i = 1, 2$, and develop R near the threshold keeping terms of the second order in ζ's, ξ's and transverse momenta. We present the difference $R_e - R$ in the form $R_e - R_0 = \Delta R_0$, where dimensionless Δ

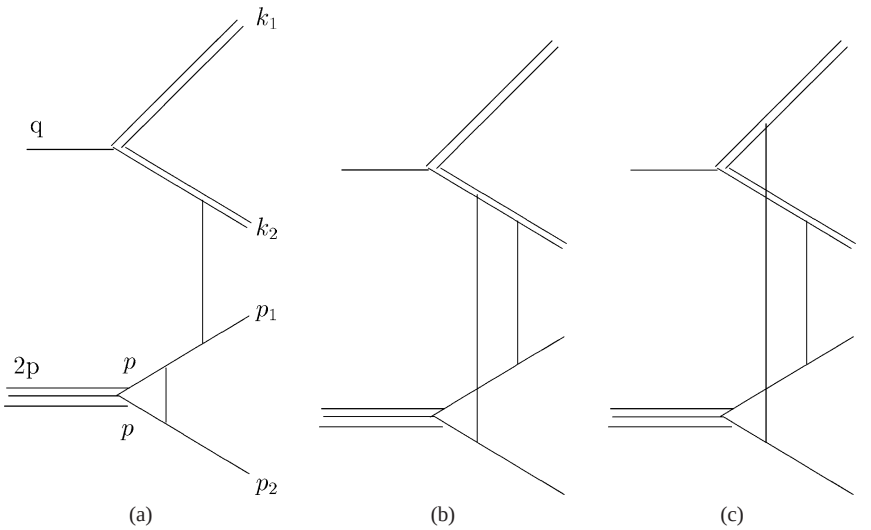

Fig. 6. Amplitudes for charm photoproduction off a meson with a single (a) and double (b), (c) gluon exchanges between light and heavy quarks. The latter are shown with double lines. Vertical lines correspond to gluonic exchanges.

measures the distance from the threshold and is supposed to be small. Finally, we rescale our variables as follows

$$\zeta_i = \tilde{\zeta}_i \sqrt{\Delta \frac{z_0^3 R_0}{M^2}}, \qquad \xi_i = \tilde{\xi}_i \sqrt{\Delta \frac{x_0^3 R_0}{m^2}}, \qquad k_{i\perp} = \tilde{k}_{i\perp} \sqrt{\Delta z_0 R_0}, \qquad p_{i\perp} = \tilde{p}_{i\perp} \sqrt{\Delta x_0 R_0}. \tag{A.3}$$

Obviously, new variables with tildes are dimensionless and of the order unity. Using this, one finds that approximately $\tilde{\zeta}_1 = -\tilde{\zeta}_2$ and $\tilde{k}_2 = -\tilde{k}_1$. So the phase volume acquires the form

$$dV = V_0 \Delta^{7/2} \frac{d\tilde{z}_1\, d\tilde{\xi}_1\, d\tilde{\xi}_2\, d^2\tilde{k}_{1\perp}\, d\tilde{p}_{1\perp}\, d\tilde{p}_{2\perp}}{\big(x_0 + \tilde{\xi}_1 \sqrt{2\Delta x_0}\big)\big(x_0 + \tilde{\xi}_2 \sqrt{2\Delta x_0}\big)} \delta\big(1 - 2\tilde{\zeta}_1^2 - \tilde{\xi}_1^2 - \tilde{\xi}_2^2 - 2\tilde{k}_{1\perp}^2 - \tilde{p}_{1\perp}^2 - \tilde{p}_{2\perp}^2\big), \tag{A.4}$$

where $V_0 = m^3 M \sqrt{z_0/2}/(2\pi)^8$.

A.2. Amplitudes

We use the Coulomb gauge for the interaction between quarks and neglect the contribution from the transverse momenta in it. Then the interaction depends only on the scaling variables, and for the transition between, say, light quarks $p_1 + p_2 \to p_1' + p_2'$ is given by

$$V(p_1, p_2 | p_1', p_2') = 4\pi\alpha_s \frac{(x_1 + x_1')(x_2 + x_2')}{(x_1 - x_1')^2}. \tag{A.5}$$

We shall assume that the initial light quarks have their momenta equal to p, so that their scaling variable is equal to unity. We omit the the common factor due to their binding into the initial target meson. Finally we consider photoproduction, so that $q^2 = 0$ and choose a system in which $q_+ = q_\perp = \mathbf{p} = 0$.

The amplitude corresponding to Fig. 6(a) is given by

$$\mathcal{A}^{(\mathrm{a})} = \frac{V(p, p | 2p - p_2, p_2) V(q - k_1, 2p - p_2 | k_2, p_1)}{(\mu^2 - (2p - p_2)^2)(m_c^2 - (q - k_1)^2)} \tag{A.6}$$

The two interactions near the threshold turn into $12\pi\alpha_s$ and $2\pi\alpha_s(z_2 - z_1)$, where we used the fact that $x_1, x_2 \ll 1$ and $z_1, z_2 \simeq 1$. For the same reason we find the two denominators as $\mu^2 - (2p - p_2)^2 \simeq 2\mu_{2\perp}^2/x_2$

and $m_c^2 - (q-k_1)^2 \simeq 2pq$. In our dimensionless variables we obtain

$$\mathcal{A}^{(a)} = -2c_1\sqrt{2z_0\Delta}\,\frac{\tilde{\xi}_1\big(x_0+\tilde{\xi}_1\sqrt{2x_0\Delta}\big)}{\mu^2+2\mu(m_c+\mu)\Delta\tilde{p}_{2\perp}^2}, \qquad c_1 = \frac{6\pi^2\alpha_s^2}{pq}. \tag{A.7}$$

The amplitude corresponding to Fig. 6(b) is

$$\mathcal{A}^{(b)} = \frac{V(q-k_1,\,p|q-k_1+p-p_1,\,p_1)V(q-k_1+p-p_1,\,p|k_2,\,p_2)}{(m_c^2-(q-k_1)^2)(m_c^2-(q-k_1+p-p_1)^2)}. \tag{A.8}$$

Near the threshold the interactions become $-4\pi\alpha_s$ and $4\pi\alpha_s$ The new denominator is

$$m_c^2-(q-k_1+p-p_1)^2 \simeq m_c^2+2(m_c+\mu)\Delta\big(\sqrt{m_c}\,\tilde{k}_1+\sqrt{\mu}\,\tilde{p}_1\big)_\perp^2. \tag{A.9}$$

At $\Delta \ll 1$ we can drop the second term. So we get

$$\mathcal{A}^{(b)} = -c_2\frac{1}{m_c^2}, \qquad c_2 = \frac{8\pi^2\alpha_s^2}{pq}. \tag{A.10}$$

Finally, we consider the amplitude of Fig. 6(c):

$$\mathcal{A}^{(c)} = \frac{V(k_1-p+p_1,\,p|k_1,\,p_1)V(k_2-p+p_2,\,p|k_2,\,p_2)}{(m_c^2-(k_1-p+p_1)^2)(m_c^2-(k_2-p+p_2)^2)}. \tag{A.11}$$

Near the threshold both interactions become approximately equal to $4\pi\alpha_s$ and both denominators to m_c^2. So the amplitude becomes

$$\mathcal{A}^{(c)} = 2c_2\frac{pq}{m_c^4} \simeq 2c_2\frac{1}{m_c^2}, \tag{A.12}$$

where we have used that near the threshold $pq \simeq m_c^2$. So the amplitudes (b) and (c) have the same order of magnitude.

A.3. Cross-sections

Now we can pass to our main goal: comparison of contributions of the three amplitudes to the total cross-section for heavy flavour production. The first thing to note is that near the threshold amplitude (a) does not interfere with (b) and (c), since $\mathcal{A}^{(a)}$ is odd in ζ_1 and $\mathcal{A}^{(b,c)}$ do not depend on ζ_1 at all. Second, since $A^{(b)}$ and $A^{(c)}$ are of the same order and structure it is sufficient to compare the contributions of $A^{(a)}$ and $A^{(b)}$. Finally, due to the fact that x_0 is small, the magnitude of contributions depends on the relation between Δ and x_0. We shall study two limiting cases: $\Delta \ll x_0$ (region A) and $\Delta \gg x_0$ (region B).

Region A refers to the production immediately above the threshold. In this case we can take $x_{1,2} \simeq x_0$. Then we find the contribution of amplitude (a) to the cross-section as

$$\sigma^{(a)} = V_0\Delta^{7/2}\frac{1}{x_0^2}\left[2c_1\sqrt{2\Delta}\,\frac{x_0}{\mu^2}^2\right]I^{(a)}, \tag{A.13}$$

where $I^{(a)}$ is a certain integral of the order unity. The contribution of the amplitude (b) to the cross-section will be

$$\sigma^{(b)} = V_0\Delta^{7/2}\frac{1}{x_0^2}\left[c_2\frac{1}{m_c^2}\right]^2 I^{(b)}, \tag{A.14}$$

where $I^{(b)}$ is another integral of the order unity. The ratio of these two cross-sections will have the order

$$\frac{\sigma^{(b)}}{\sigma^{(a)}} \sim \frac{\mu^2(m_c+\mu)^2}{m_c^4\Delta} \sim \frac{\mu^2}{m_c^2\Delta} \sim \frac{x_0^2}{\Delta}. \tag{A.15}$$

Thus immediately above the threshold the contribution from amplitudes (b) and (c) dominate. However with the growth of Δ, in the region $x_0^2 \ll \Delta$ (and $\ll x_0$ to still remain in region A) the contribution of amplitudes of (b) and (c) become suppressed by factor μ/m_c.

In region B we can approximate $x_{1,2} \simeq \tilde{\xi}_{1,2}\sqrt{2x_0\Delta}$. To avoid logarithmic divergence in $\tilde{\xi}_{1,2}$ we cutoff the integration region from below at values of the order $\sqrt{x_0/\Delta}$. We also note that the integral over $\tilde{p}_{1\perp}$ appearing in the contribution of amplitude (a) is well convergent at values of $\tilde{p}_{1\perp}^2 \sim x_0/\Delta$ so that we may neglect $\tilde{p}_{1\perp}^2$ in the argument of the δ-function and separate the integration over $\tilde{p}_{1\perp}$ as a factor

$$\int \frac{d^2\tilde{p}_{1\perp}}{[\mu^2 + 2\mu(m_c+\mu)\Delta\tilde{p}_{2\perp}^2]^2} = \frac{\pi}{2\mu^3(m_c+\mu)\Delta}. \tag{A.16}$$

We find the cross-section from $A^{(a)}$ as

$$\sigma^{(a)} = V_0\Delta^{5/2}\frac{1}{2x_0}\left[2c_1 2\Delta\sqrt{x_0}\right]^2\frac{\pi}{2\mu^3(m_c+\mu)\Delta}J^{(a)}, \tag{A.17}$$

where $J^{(a)}$ is an integral of the order $\ln(x_0/\Delta)$. The cross-section from $A^{(b)}$ is found to be

$$\sigma^{(b)} = V_0\Delta^{5/2}\frac{1}{2x_0}\left[c_2\frac{1}{m_c^2}\right]^2 J^{(b)} \tag{A.18}$$

with $J^{(b)}$ an integral of the order $\ln^2(x_0/\Delta)$.

The ratio of the two cross-section turns out to be of the same order up to a logarithmic factor

$$\frac{\sigma^{(b)}}{\sigma^{(a)}} \sim \frac{\mu^2(m_c+\mu)^2}{m_c^4\Delta}\ln\frac{\Delta}{x_0} \sim \frac{\mu^2}{m_c^2\Delta}\ln\frac{m_c\Delta}{\mu} \sim \frac{x_0^2}{\Delta}\ln\frac{\Delta}{x_0}, \tag{A.19}$$

and so the contribution of amplitude (a) clearly dominates in region B, where $\Delta \gg x_0$. The suppression factor for the contribution of the amplitudes (b) and (c) with double gluon exchange is found to be $m_c^2/(\mu^2\Delta)$. With $m_c/\mu \sim 5$ it is of the order 25Δ. Taking into account that double gluon exchange involves a coupling constant at the heavy flavour mass scale will add a factor $\sim$3 more. So in the end we find a suppression factor of the order 75Δ, which implies that at a distance of 0.3 GeV from the threshold the contribution of the double gluon exchange drops by a factor $\sim$3.

A.4. Bound states

One may wonder if the production cross-section is dominated by the formation of final bound states, via diagrams as Fig. 7(a), which looks as quark rearrangement without any gluon exchange [4]. However, one has to recall that in the bound state of a light and a heavy quark (D-meson) the typical configuration requires $p_{i+}/l_{i+} = \mu/m_D$ and $k_{i+}/l_{i+} = m_c/m_D$, where we neglect the binding taking $m_D = m_c + \mu$. The initial light

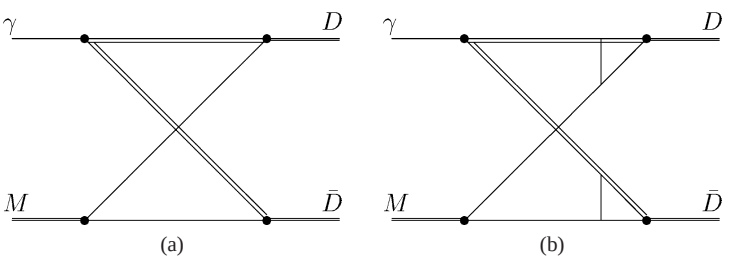

Fig. 7. Amplitudes for the $D\bar{D}$ photoproduction off a meson. Diagram (a) is equivalent to diagram (b), which shows how the produced quarks aquire their momenta appropriate for the binding. Notations are as in Fig. 6.

quarks have however $p_{i+} = p_+$. So for their binding into D-mesons, they have to diminish their longitudinal momenta by at least two hard gluon exchanges, as shown in Fig. 2(b). But the process in Fig. 2(b) contributes actually a part of the cross-section generated by the amplitude $A^{(c)}$ studied in the preceding subsection, which corresponds to the immediate binding of the open charm into D-mesons. Above the threshold of the open charm production its contribution can only be smaller than the total rate of open charm production. True, immediately below this threshold, at distances of the order of the binding energy, this mechanism is obviously the only one that contributes, in agreement with the estimates above for very small Δ's. However, as we have seen, with the growth of Δ the strength of multiple interactions between light and heavy quarks necessary to produce them in a state appropriate for their binding rapidly goes down. With them goes down also the correspondiing part of the cross-section due to immediate binding.

References

[1] M. Franz, K. Goeke, M.V. Polyakov, Phys. Rev. D 62 (2000) 074024.
[2] M.A. Braun, B. Vlahovic, hep-ph/0209261.
[3] S.J. Brodsky, E. Chudakov, P. Hoyer, J.M. Laget, Phys. Lett. B 498 (2001) 23.
[4] B. Kopelovich, private communication.
[5] M. Glueck, E. Reya, A. Vogt, Z. Phys. C 67 (1995) 433.
[6] BCDMS Collaboration, Z. Phys. C 63 (1994) 29.
[7] Y.D. Bayukov, et al., Phys. Rev. C 20 (1979) 764;
N.A. Nikiforov, et al., Phys. Rev. C 22 (1980) 700.
[8] J. Smith, W.L. van Neerven, Nucl. Phys. B 374 (1992) 36.
[9] J. Andersen, et al., hep-ph/0312333.